

# A Note on Kinematic Flow and Differential Equations for Two-Site One-Loop Graph in FRW Spacetime

---

**Yanfeng Hang**<sup>a</sup>

<sup>a</sup>*Department of Physics and Astronomy,  
Northwestern University, Evanston, IL 60208, USA*

*E-mail:* [yfhang@northwestern.edu](mailto:yfhang@northwestern.edu)

**ABSTRACT:** In this study, we investigate the canonical differential equations governing the two-site one-loop wavefunction coefficient in conformally-coupled scalar theory within a general FRW cosmology. By utilizing relative twisted cohomology and integration by parts, we systematically derive these equations, providing a solid foundation for further analysis. Moreover, we extend the kinematic flow framework to the one-loop level, efficiently deriving the differential equations graphically through the family trees generated by tube graphs, which are associated with the singularities of the system. This approach provides valuable insights into the dynamical behavior of the differential system for the cosmological wavefunction coefficient at the loop level.

---

## Contents

<b>1 Motivation and Background Setup</b>	<b>1</b>
<b>2 Wavefunction for Two-site One-loop Graph and Differential Equations</b>	<b>4</b>
<b>3 Kinematic Flow for Two-site One-loop Graph</b>	<b>7</b>
<b>4 Conclusion and Outlook</b>	<b>14</b>
<b>A The Derivation of Two-site One-loop DEs from IBP</b>	<b>15</b>
<b>B Differential Equations for Two-site Two-loop Graph</b>	<b>19</b>

---

## 1 Motivation and Background Setup

The investigation of differential equations related to the wavefunction coefficient for two-site one-loop graph in the Friedmann-Robertson-Walker (FRW) spacetime is essential for advancing our understanding of cosmological dynamics. In this work, we utilize relative twisted cohomology alongside integration by parts (IBP) to derive these equations. A key feature of our approach is the extension of kinematic flow to the one-loop level, which we represent the singularities of the differential system as tube graphs. This methodology enables the efficient derivation of differential equations with uniformly transcendental weights from the family trees generated by the tube graphs.

We first consider the model of conformally-coupled scalar fields with non-conformal polynomial interaction terms in a general FRW cosmology [1–4]. The action of this theory defined in a  $(d+1)$ -dimensional spacetime is expressed as follows:

$$S_{\text{FRW}} = - \int d^d x \int_{-\infty}^0 d\eta \sqrt{-g} \left( \frac{1}{2} g^{\alpha\beta} \partial_\alpha \phi \partial_\beta \phi + \frac{1}{2} \xi R \phi^2 + \sum_{n \geq 3} \frac{\lambda_n}{n!} \phi^n \right), \quad (1.1)$$

where the FRW metric and the conformal coupling constant  $\xi$  are defined as follows:

$$ds^2 = g_{\alpha\beta} dx^\alpha dx^\beta = a^2(\eta) \left( -d\eta^2 + dx^j dx_j \right), \quad \xi = \frac{d-1}{4d}, \quad (1.2)$$

with the index  $j$  spans the spatial dimensions i.e.,  $j = 1, \dots, d$ . Then, by imposing the following conformal transformations:

$$g_{\alpha\beta} \rightarrow [a(\eta)]^2 g_{\alpha\beta}, \quad \phi \rightarrow [a(\eta)]^{-\Delta} \phi, \quad (1.3)$$

with the conformal weight  $\Delta = (d - 1)/2$ , we can further rewrite the action (1.1) as the action of a massless scalar field living in the  $(d+1)$ -dimensional Minkowski (flat) spacetime:

$$S_{\text{Min}} = - \int d^d x d\eta \left[ \frac{1}{2} (\partial\phi)^2 + \sum_{n \geq 3} \frac{\lambda_n(\eta)}{n!} \phi^n \right], \quad (1.4)$$

where the time-dependent coupling  $\lambda_n(\eta)$  is defined as follows:

$$\lambda_n(\eta) \equiv \lambda_n[a(\eta)]^{2-(n-2)\Delta}. \quad (1.5)$$

Now, we provide a brief review of the cosmological wavefunction coefficients. These coefficients describe the amplitude for different configurations of fields in the early universe and encode crucial information about cosmological fluctuations. It can be derived from the path integral formalism, where the wavefunction  $\Psi[\varphi]$  is obtained by summing over all possible field configurations  $\varphi(x)$  in a given cosmological background. Specifically, the cosmological wavefunction  $\Psi[\varphi]$  can be expressed as a path integral over the field configurations:

$$\Psi[\phi] = \int_{\varphi(-\infty^+) = 0}^{\varphi(0) = \phi} \mathcal{D}\phi e^{iS[\varphi]}, \quad (1.6)$$

where  $S[\varphi]$  is the action of the field  $\varphi$  as given in eq. (1.4) and the integral is performed over all field configurations. And  $|\Psi[\phi]|^2$  provides the physical meaning of the probability density for spatial field configurations. Thus, the equal-time  $n$ -point correlation function for  $\phi$  can be written as:

$$\langle \phi(\mathbf{x}_1) \cdots \phi(\mathbf{x}_n) \rangle = \int \mathcal{D}\phi \phi(\mathbf{x}_1) \cdots \phi(\mathbf{x}_n) |\Psi[\phi]|^2. \quad (1.7)$$

The wavefunction can also be expanded in terms of its coefficients, which are related to cosmological correlation functions. For example, expanding  $\Psi[\phi]$  perturbatively gives:

$$\Psi[\phi] = \exp \left\{ - \sum_{n \geq 2} \frac{1}{n!} \int \prod_{i=1}^n \frac{d^d \mathbf{k}_i}{(2\pi)^d} \phi_{\mathbf{k}_i} \left[ \psi_n(\{\mathbf{k}_j\}) (2\pi)^d \delta^{(d)} \left( \sum_{\ell=1}^n \mathbf{k}_\ell \right) \right] \right\}, \quad (1.8)$$

where  $\psi_n(\{\mathbf{k}_j\})$  are the cosmological wavefunction coefficients, encoding the interactions between  $n$ -point fluctuations of the field. The leading term  $\psi_2(\mathbf{k}_1, \mathbf{k}_2)$  corresponds to the two-point correlation function, higher-order coefficients, like  $\psi_3(\mathbf{k}_1, \mathbf{k}_2, \mathbf{k}_3)$ , capture interactions between modes and lead to non-Gaussianities.

The path integral can be performed diagrammatically in the usual way with Feynman graphs, which consist of a set  $\mathcal{V}$  of vertices and  $\mathcal{E}$  of edges. Each diagram corresponds to a specific contribution to the perturbative expansion of the wavefunction. The Feynman rules can be derived as: (i). Vertices represent interaction points, where several fields interact. The form of the vertex  $V_v$  is determined by the interaction terms in the action. In the case of a scalar field with non-derivative polynomial interactions,  $V_v$  is just a function of the coupling constant and does not depend on the spatial momenta of the external states attached to the vertex. (ii). The bulk-to-boundary propagators  $K_v(E_v; \eta_v)$ , associated with a vertex  $v$ ,

correspond to the propagation of a field from a bulk vertex to the boundary of spacetime, and it takes the form:

$$K_v(E_v; \eta_v) = e^{iE_v \eta_v}, \quad (1.9)$$

where  $E_v = \sum_i |\mathbf{k}_i|$  denotes the sum of the energies of all  $i$  external legs connected to the vertex  $v$ . (iii). The bulk-to-bulk propagators  $G_e(E_e; \eta_{v_e}, \eta_{v'_e})$ , associated with an edge  $e$ , describe the propagation of fields between two interaction vertices  $(v_e, v'_e)$  located at different times. We can express this propagator as follows:

$$G_e(E_e; \eta_{v_e}, \eta_{v'_e}) = -\frac{1}{2E_e} \left\{ \exp[iE_e(\eta_{v_e} + \eta_{v'_e})] - \exp[-iE_e(\eta_{v_e} - \eta_{v'_e})] \theta(\eta_{v_e} - \eta_{v'_e}) \right. \\ \left. - \exp[-iE_e(\eta_{v'_e} - \eta_{v_e})] \theta(\eta_{v'_e} - \eta_{v_e}) \right\}, \quad (1.10)$$

where  $E_e = |\mathbf{k}_e|$  represent the energy of an internal line  $e$ . These propagators incorporate the causal structure of the theory, accounting for the time evolution of field modes as they interact within the bulk. Given these ingredients, each Feynman diagram is constructed by assigning a bulk-boundary propagator  $K_v$  to each vertex connected to the boundary and a bulk-bulk propagator  $G_e$  to each internal line connecting two vertices.

Finally, we assume that the scale factor  $a(\eta)$  in eq. (1.2) takes the following power-law form [5–7]:

$$a(\eta) = \left( \frac{\eta_0}{\eta} \right)^{1+\varepsilon}, \quad (1.11)$$

where  $\eta_0$  is an arbitrary time scale in order to normalize the scale factor and the parameter  $\varepsilon = 0, -1, -2, -3$  corresponding to the dS, flat, radiation and matter dominated universe respectively. Further, in the study of wavefunction coefficients, the twist factor  $\varepsilon$  denotes the exponent of the twist associated with those coefficients, allowing one to examine the properties of these coefficients while managing potential singularities. Moreover, the twist factor  $\varepsilon$  is related to the relative twisted cohomology [8, 9] and intersection theory which facilitate the analysis of correlators and perturbations in FRW universe.

In the case of a power-law form (1.11), we can analyze and compute the wavefunction coefficient in FRW spacetime. The corresponding Feynman rules need slight modifications, where the bulk-to-boundary propagator (1.9) and bulk-to-bulk propagator (1.10) remain unchanged from their flat spacetime forms. As for the vertices, the coupling of the non-polynomial interaction term in (1.1) can be expressed in energy space via the Fourier transformation

$$\lambda_n(\eta) = N \int_0^\infty dx x^{a(1+\varepsilon)-1} e^{ix\eta} \equiv N \int_0^\infty dx \bar{\lambda}_n(x) e^{ix\eta}, \quad (1.12)$$

where  $x$  is of the same order as energy,  $N$  is a normalization factor and  $a = 2 - (n - 2)\Delta$  with  $\Delta = (d-1)/2$ . Therefore, the  $n$ -site  $\ell$ -loop wavefunction coefficient in FRW cosmology is obtained by shifting the its flat-space form over external energies:

$$\psi_{n, \text{FRW}}^{(\ell)} = \int_0^\infty \prod_{v \in \mathcal{V}} dx_v \bar{\lambda}_{n,v}(x) \psi_{n, \text{Mink}}^{(\ell)}(X_v + x_v, Y_e), \quad (1.13)$$

where the flat-space wavefunction is given by

$$\psi_{n,\text{Mink}}^{(\ell)}(X_v, Y_e) = \int_{-\infty}^0 \prod_{v \in \mathcal{V}} d\eta_v e^{iX_v \eta_v} \prod_{e \in \mathcal{E}} G_e(Y_e; \eta_{v_e}, \eta_{v'_e}). \quad (1.14)$$

In eqs. (1.13)-(1.14), the variables  $X_v$  and  $Y_e$  denote the total energies flowing from a vertex  $v$  to the boundary and the energies of internal lines  $e$  respectively.

## 2 Wavefunction for Two-site One-loop Graph and Differential Equations

We consider  $\phi^3$  theory in (3+1)-dimensional spacetime, the wavefunction coefficient for two-point two-site one-loop receives the contribution from a single one-particle irreducible (1PI) graph as shown in fig. 2.

As illustrated in ref. [1], the wavefunction coefficient for a graph can be obtained by summing over all possible ways of iteratively dividing the graph into connected subgraphs, each associated with the inverse of the sum of its external energies. For the two-site one-loop graph, there are two distinct ways to divide the graph into connected subgraphs, with the wavefunction coefficients for the two subgraphs being

$$\psi_{2,\text{Mink}}'^{(1)} = \frac{1}{X_1 + X_2} \times \frac{1}{X_1 + X_2 + 2Y_1} \times \frac{1}{X_1 + Y_1 + Y_2} \times \frac{1}{X_2 + Y_1 + Y_2}, \quad (2.1a)$$

$$\psi_{2,\text{Mink}}''^{(1)} = \frac{1}{X_1 + X_2} \times \frac{1}{X_1 + X_2 + 2Y_2} \times \frac{1}{X_1 + Y_1 + Y_2} \times \frac{1}{X_2 + Y_1 + Y_2}. \quad (2.1b)$$

Summing over the two contributions in eq. (2.1), we can obtain the full wavefunction coefficient of the two-site one-loop graph as:

$$\begin{aligned} \psi_{2,\text{Mink}}^{(1)} &= \psi_{2,\text{Mink}}'^{(1)} + \psi_{2,\text{Mink}}''^{(1)} \\ &= \frac{2(X_1 + X_2 + Y_1 + Y_2)}{(X_1 + X_2)(X_1 + X_2 + 2Y_1)(X_1 + X_2 + 2Y_2)(X_1 + Y_1 + Y_2)(X_2 + Y_1 + Y_2)}. \end{aligned} \quad (2.2)$$

Then, in order to derive the one-loop wavefunction coefficient in FRW cosmology,  $\psi_{2,\text{FRW}}^{(1)}$ , we can modify its corresponding flat-space wavefunction coefficient,  $\psi_{2,\text{Mink}}^{(1)}$ . This is achieved by shifting the external energies from  $\psi_{2,\text{Mink}}^{(1)}$ , specifically imposing the following transformations:  $(X_1, X_2) \rightarrow (X_1 + x_1, X_2 + x_2)$ . Following these energy shifts, we can

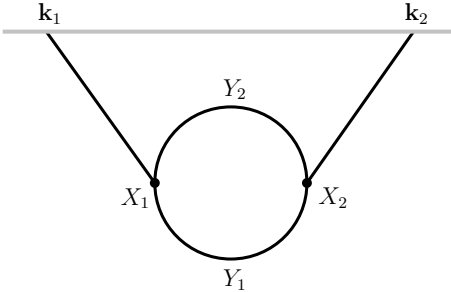


**Figure 1.** The Feynman diagram for two-site one-loop wavefunction coefficient of  $\phi^3$  theory.

incorporate the twist term  $(x_1 x_2)^\varepsilon$ , which regularizes the integrand by controlling the behavior near singularities through the parameter  $\varepsilon$ ,

$$\begin{aligned}\psi_{2,\text{FRW}}^{(1)} &= \int dx_1 \wedge dx_2 (x_1 x_2)^\varepsilon \psi_{2,\text{Min}}^{(1)} \Big|_{\substack{X_1 \rightarrow X_1 + x_1 \\ X_2 \rightarrow X_2 + x_2}} \\ &= \int dx_1 \wedge dx_2 (T_1 T_2)^\varepsilon \left[ \frac{1}{L_1 L_2 D_3} \left( \frac{1}{D_1} + \frac{1}{D_2} \right) \right] \equiv \int (T_1 T_2)^\varepsilon \Omega_{\mathcal{P}}^2, \end{aligned}\quad (2.3)$$

where we have defined:

$$\begin{aligned}T_1 &= x_1, & T_2 &= x_2, \\ L_1 &= X_1 + x_1 + Y_1 + Y_2, & L_2 &= X_2 + x_2 + Y_1 + Y_2, \\ D_1 &= X_1 + X_2 + x_1 + x_2 + 2Y_1, & D_2 &= X_1 + X_2 + x_1 + x_2 + 2Y_2, \\ D_3 &= X_1 + X_2 + x_1 + x_2. \end{aligned}\quad (2.4)$$

The divisors in eq. (2.4) are expressed in the linear form corresponding to seven hyperplanes,  $\{T_i, L_j, D_k\} = 0$ , as arranged in  $(x_1, x_2)$ -plane shown in fig. 2. The branch surfaces,  $\{T_1, T_2\} = 0$ , represent the twisted singularities within the integrand, which are regulated by the parameter  $\varepsilon$ . While the hyperplanes  $\{L_i, D_j\} = 0$  associated with the relative singularities. The overall analytic structure of the integrals is primarily determined by the way the surfaces  $\{T_i, L_j, D_k\} = 0$  intersect with one another, as these intersections dictate the behavior and singularities of the system.

The number of independent master integrals is equal to the number of chambers (bounded regions) enclosed by the hyperplanes [10, 11]. We find that the hyperplane arrangement in fig. 2 can be decomposed into three subsystems of hyperplane arrangements. These three subsystems all share the common hyperplanes  $\{T_i, L_j\} = 0$  with  $(i, j) = 1, 2$ , while each subsystem contains a set of distinct diagonally placed hyperplanes, also denoted by  $D_i = 0$  with  $i = 1, 2, 3$ . As a result, we can count a total of twelve chambers in fig. 2, with each chamber is a canonical form [12] of triangle from hyperplane arrangement. According to refs. [6, 7], each chamber corresponds to a distinct wavefunction. In each subsystem of

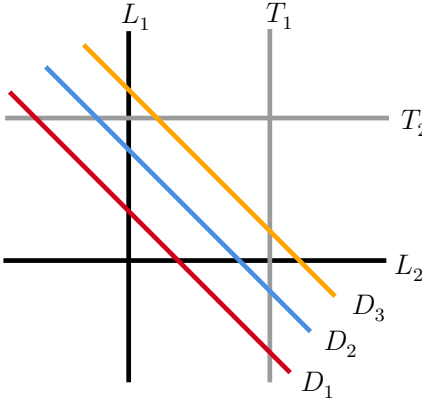


**Figure 2.** Hyperplane arrangement for the two-site one-loop wavefunction coefficient.

hyperplane arrangements, there is one “parent” function  $\mathcal{P}_i$  and three “source” functions  $\mathcal{F}_i, \tilde{\mathcal{F}}_i, \mathcal{Q}_i$ , defined as follows:

$$\{L_1, L_2, D_i\} = 0 : \quad \mathcal{P}_i = \int (T_1 T_2)^\varepsilon \left( \text{dlog} \frac{L_1}{D_i} \wedge \text{dlog} \frac{L_2}{D_i} \right) \equiv \int (T_1 T_2)^\varepsilon \Omega_{\mathcal{P}_i}^2, \quad (2.5a)$$

$$\{T_1, L_2, D_i\} = 0 : \quad \mathcal{F}_i = \int (T_1 T_2)^\varepsilon \left( \text{dlog} \frac{T_1}{L_2} \wedge \text{dlog} \frac{T_1}{D_i} \right) \equiv \int (T_1 T_2)^\varepsilon \Omega_{\mathcal{F}_i}^2, \quad (2.5b)$$

$$\{T_2, L_1, D_i\} = 0 : \quad \tilde{\mathcal{F}}_i = \int (T_1 T_2)^\varepsilon \left( \text{dlog} \frac{T_2}{D_i} \wedge \text{dlog} \frac{T_2}{L_1} \right) \equiv \int (T_1 T_2)^\varepsilon \Omega_{\tilde{\mathcal{F}}_i}^2, \quad (2.5c)$$

$$\{T_1, T_2, D_i\} = 0 : \quad \mathcal{Q}_i = \int (T_1 T_2)^\varepsilon \left( \text{dlog} \frac{T_1}{D_i} \wedge \text{dlog} \frac{T_2}{D_i} \right) \equiv \int (T_1 T_2)^\varepsilon \Omega_{\mathcal{Q}_i}^2, \quad (2.5d)$$

where  $i = 1, 2, 3$ , and by defining  $\Omega^2 \equiv \bar{\Omega}^2 dx_1 \wedge dx_2$ , we can further derive

$$\begin{aligned} \bar{\Omega}_{\mathcal{P}_1}^2 &= \frac{-2Y_2}{L_1 L_2 D_1}, & \bar{\Omega}_{\mathcal{F}_1}^2 &= \frac{X_1 + Y_1 - Y_2}{T_1 L_2 D_1}, & \bar{\Omega}_{\tilde{\mathcal{F}}_1}^2 &= \frac{X_2 + Y_1 - Y_2}{T_2 L_1 D_1}, & \bar{\Omega}_{\mathcal{Q}_1}^2 &= \frac{X_1 + X_2 + 2Y_1}{T_1 T_2 D_1}, \\ \bar{\Omega}_{\mathcal{P}_2}^2 &= \frac{-2Y_1}{L_1 L_2 D_2}, & \bar{\Omega}_{\mathcal{F}_2}^2 &= \frac{X_1 - Y_1 + Y_2}{T_1 L_2 D_2}, & \bar{\Omega}_{\tilde{\mathcal{F}}_2}^2 &= \frac{X_2 - Y_1 + Y_2}{T_2 L_1 D_1}, & \bar{\Omega}_{\mathcal{Q}_2}^2 &= \frac{X_1 + X_2 + 2Y_2}{T_1 T_2 D_2}, \\ \bar{\Omega}_{\mathcal{P}_3}^2 &= \frac{-2(Y_1 + Y_2)}{L_1 L_2 D_3}, & \bar{\Omega}_{\mathcal{F}_3}^2 &= \frac{X_1 - Y_1 - Y_2}{T_1 L_2 D_3}, & \bar{\Omega}_{\tilde{\mathcal{F}}_3}^2 &= \frac{X_2 - Y_1 - Y_2}{T_2 L_1 D_3}, & \bar{\Omega}_{\mathcal{Q}_3}^2 &= \frac{X_1 + X_2}{T_1 T_2 D_3}. \end{aligned} \quad (2.6)$$

However, the twelve bounded chambers have actually been overcounted. Considering the two form  $\Omega_{\mathcal{P}}^2$  given in eq. (2.3) and the sum of three 2-forms  $\sum_i \Omega_{\mathcal{P}_i}^2$  given in eq. (2.5a), we find they are equivalent in twist cohomology [11, 13]. In fact, the equivalence in twist cohomology comes from the fact that the two rational forms  $\Omega_{\mathcal{P}}^2$  and  $\sum_i \Omega_{\mathcal{P}_i}^2$  only differ by the covariant derivative of a 1-form, and they represent the same cohomology class. Precisely:

$$\Omega_{\mathcal{P}}^2 - \sum_{i=1}^3 \Omega_{\mathcal{P}_i}^2 = \nabla_{\omega} \alpha, \quad (2.7)$$

where  $\alpha$  is some 1-form and the covariant derivative is defined as follows:

$$\nabla_{\omega} = d + \omega \wedge, \quad \omega = \varepsilon \left( \frac{dx_1}{x_1} + \frac{dx_2}{x_2} \right). \quad (2.8)$$

Constructing this exact form  $\alpha$  is straightforward, conforming that  $\Omega_{\mathcal{P}}^2$  and  $\sum_i \Omega_{\mathcal{P}_i}^2$  are cohomologically equivalent. Therefore, there are ten independent bounded chambers, each corresponding to a distinct function. The number of those functions/chambers is equal to the number of independent master integrals, which belong to an integral family **I**:

$$\mathbf{I} = (\mathcal{P}, \mathcal{F}_1, \mathcal{F}_2, \mathcal{F}_3, \tilde{\mathcal{F}}_1, \tilde{\mathcal{F}}_2, \tilde{\mathcal{F}}_3, \mathcal{Q}_1, \mathcal{Q}_2, \mathcal{Q}_3)^T. \quad (2.9)$$

It was proposed in ref. [14] that a canonical basis of master integrals can be constructed, where each integral has uniform transcendental weight (UT). Hence, the basis **I** satisfies a linear system of differential equations in a simple canonical form, governed by a first-order equation:

$$d\mathbf{I} = \varepsilon \tilde{A} \mathbf{I}, \quad \tilde{A} = \sum_i a_i \text{dlog}[\ell_i(X_a, Y_b)], \quad (2.10)$$

where  $a_i$  is a  $n \times n$  constant matrix and  $\ell_i$ 's represent the (symbol) letters which are the rational or algebraic functions of kinematic variables  $\{X_a, Y_b\}$ . Further, the transformation matrix  $\tilde{A}$  obeys the following integrability conditions:

$$d\tilde{A} = 0, \quad \tilde{A} \wedge \tilde{A} = 0. \quad (2.11)$$

In Appendix A, we have computed all canonical differential equations by using the method of IBP and we summarized our results as:

$$\begin{aligned} d\mathcal{P} &= \varepsilon \left[ \left( \mathcal{P} - \sum_{i=1}^3 \mathcal{F}_i \right) d\log(X_1 + Y_1 + Y_2) + \left( \mathcal{P} - \sum_{i=1}^3 \tilde{\mathcal{F}}_i \right) d\log(X_2 + Y_1 + Y_2) \right. \\ &\quad + \mathcal{F}_1 d\log(X_1 + Y_1 - Y_2) + \tilde{\mathcal{F}}_1 d\log(X_2 + Y_1 - Y_2) \\ &\quad + \mathcal{F}_2 d\log(X_1 - Y_1 + Y_2) + \tilde{\mathcal{F}}_2 d\log(X_2 - Y_1 + Y_2) \\ &\quad \left. + \mathcal{F}_3 d\log(X_1 - Y_1 - Y_2) + \tilde{\mathcal{F}}_3 d\log(X_2 - Y_1 - Y_2) \right], \\ d\mathcal{F}_1 &= \varepsilon [\mathcal{F}_1 d\log(X_1 + Y_1 - Y_2) + (\mathcal{F}_1 - \mathcal{Q}_1) d\log(X_2 + Y_1 + Y_2) + \mathcal{Q}_1 d\log(X_1 + X_2 + 2Y_1)], \\ d\tilde{\mathcal{F}}_1 &= \varepsilon [\tilde{\mathcal{F}}_1 d\log(X_2 + Y_1 - Y_2) + (\tilde{\mathcal{F}}_1 - \mathcal{Q}_1) d\log(X_1 + Y_1 + Y_2) + \mathcal{Q}_1 d\log(X_1 + X_2 + 2Y_1)], \\ d\mathcal{F}_2 &= \varepsilon [\mathcal{F}_2 d\log(X_1 - Y_1 + Y_2) + (\mathcal{F}_2 - \mathcal{Q}_2) d\log(X_2 + Y_1 + Y_2) + \mathcal{Q}_2 d\log(X_1 + X_2 + 2Y_2)], \\ d\tilde{\mathcal{F}}_2 &= \varepsilon [\tilde{\mathcal{F}}_2 d\log(X_2 - Y_1 + Y_2) + (\tilde{\mathcal{F}}_2 - \mathcal{Q}_2) d\log(X_1 + Y_1 + Y_2) + \mathcal{Q}_2 d\log(X_1 + X_2 + 2Y_2)], \\ d\mathcal{F}_3 &= \varepsilon [\mathcal{F}_3 d\log(X_1 - Y_1 - Y_2) + (\mathcal{F}_3 - \mathcal{Q}_3) d\log(X_2 + Y_1 + Y_2) + \mathcal{Q}_3 d\log(X_1 + X_2)], \\ d\tilde{\mathcal{F}}_3 &= \varepsilon [\tilde{\mathcal{F}}_3 d\log(X_2 - Y_1 - Y_2) + (\tilde{\mathcal{F}}_3 - \mathcal{Q}_3) d\log(X_1 + Y_1 + Y_2) + \mathcal{Q}_3 d\log(X_1 + X_2)], \\ d\mathcal{Q}_1 &= 2\varepsilon \mathcal{Q}_3 d\log(X_1 + X_2 + 2Y_1), \\ d\mathcal{Q}_2 &= 2\varepsilon \mathcal{Q}_2 d\log(X_1 + X_2 + 2Y_2), \\ d\mathcal{Q}_3 &= 2\varepsilon \mathcal{Q}_1 d\log(X_1 + X_2). \end{aligned} \quad (2.12)$$

### 3 Kinematic Flow for Two-site One-loop Graph

In this section, we begin by introducing the graphical method to represent the letters associated with differential equations. To ensure that all letters are captured, a marking, specifically a cross sign, is placed on each internal line. The letters are then depicted as the “connected tubes”, which are formed by encircling both the vertices and the marked internal lines in the graph. Importantly, each tube must contain at least one vertex. A letter is assigned to each tube, calculated as the sum of the vertex energies enclosed within the tube, along with the energies of the internal lines that pass through it. For tubes that intersect an internal line and enclose the corresponding cross, the sign of the internal energy is inverted. Consequently, the letters for the two-site one-loop graph are summarized in table 1. For convenience, we have defined  $l_i \equiv d\log \ell_i$  and refer to  $l_i$  as the letters, this terminology will be used consistently throughout this section and in subsequent sections.

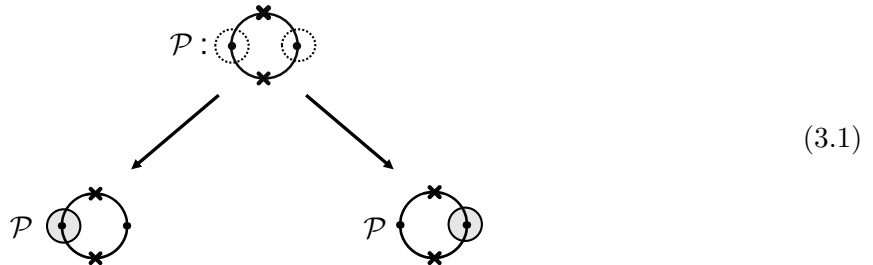
Initially, we focus on the graph of the parent function  $\mathcal{P}$ . We use dashed lines to enclose each vertex, representing the “seeds” that serve as fundamental building blocks for

$l_1$		$\text{dlog}(X_1 + Y_1 + Y_2)$	$l_2$		$\text{dlog}(X_2 + Y_1 + Y_2)$
$l_3$		$\text{dlog}(X_1 + Y_1 - Y_2)$	$l_4$		$\text{dlog}(X_2 + Y_1 - Y_2)$
$l_5$		$\text{dlog}(X_1 - Y_1 + Y_2)$	$l_6$		$\text{dlog}(X_2 - Y_1 + Y_2)$
$l_7$		$\text{dlog}(X_1 - Y_1 - Y_2)$	$l_8$		$\text{dlog}(X_2 - Y_1 - Y_2)$
$l_9$		$\text{dlog}(X_1 + X_2 + 2Y_1)$	$l_{10}$		$\text{dlog}(X_1 + X_2 + 2Y_2)$
$l_{11}$		$\text{dlog}(X_1 + X_2)$			

**Table 1.** The alphabet of two-site one-loop wavefunction coefficient where  $l_i \equiv \text{dlog } \ell_i$ .

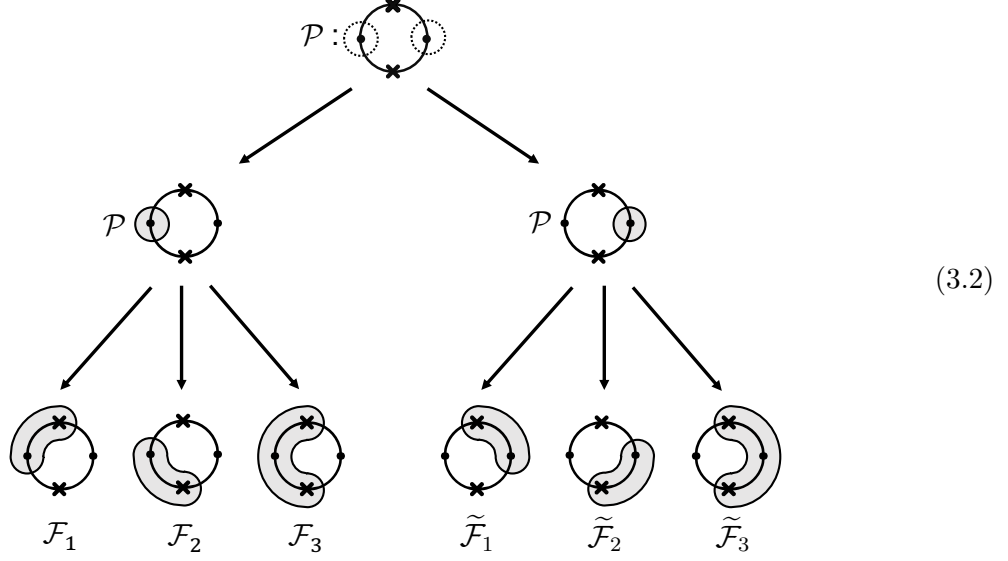
constructing a more complex structure. By activating these seeds one by one, we create the corresponding family tree, where each activation signifies the emergence of a new branch. Each activated tube corresponds to a letter in the differential equation, which facilitates the derivation of the equations governing our system. These letters represent different components of the differential equations we aim to derive. As we proceed with the activation process, we will observe how each subsequent activation generates additional branches and letters, thereby expanding our family tree and deepening our understanding of the underlying mathematical structure. With each new branch, we gain insights into the relationships between the various components of the differential equations, elucidating the overall behavior of the system represented by  $\mathcal{P}$ .

Now, we will construct the family tree for  $\mathcal{P}$  step by step. First, activating the tubes of  $\mathcal{P}$  generates two branches, each corresponding to a distinct letter,



where for each graph in the tree, we have also assigned the function corresponding to the graph tubing. Next, each activated tube in (3.1) that does not contain a cross sign can “grow” to enclose all of its adjacent crosses. Each possible way this growth occurs generates

new branches of the family tree:

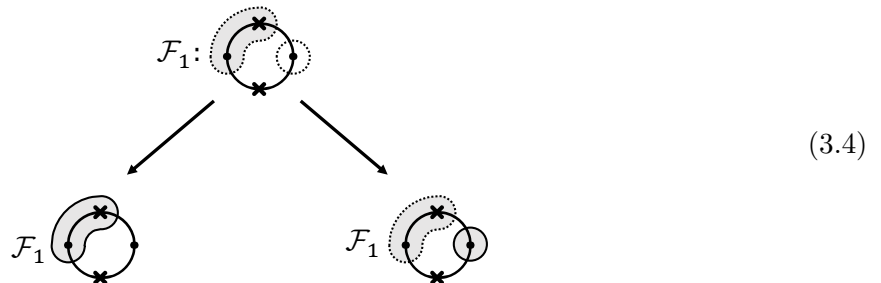


where we have assigned the source functions  $\{\mathcal{F}_i\}$  and  $\{\tilde{\mathcal{F}}_i\}$  corresponding to the graphs in the third line of eq. (3.2). Finally, we multiply the letter by its corresponding function associated to the graph in eq. (3.1) minus the functions associated to all of its descendant graphs, with an overall constant factor  $\varepsilon$ . That yields to the differential equation according to the full family tree (3.2):

$$\begin{aligned}
 d\mathcal{P} &= \varepsilon \left[ \left( \mathcal{P} - \sum_{i=1}^3 \mathcal{F}_i \right) l_1 + \left( \mathcal{P} - \sum_{i=1}^3 \tilde{\mathcal{F}}_i \right) l_2 + \sum_{i=1}^3 \mathcal{F}_i l_{2i+1} + \sum_{i=1}^3 \tilde{\mathcal{F}}_i l_{2i+2} \right] \\
 &= \varepsilon \left[ \mathcal{P}(l_1 + l_2) + \mathcal{F}_1(l_3 - l_1) + \tilde{\mathcal{F}}_1(l_4 - l_2) + \mathcal{F}_2(l_5 - l_1) + \tilde{\mathcal{F}}_2(l_6 - l_2) \right. \\
 &\quad \left. + \mathcal{F}_3(l_7 - l_1) + \tilde{\mathcal{F}}_3(l_8 - l_2) \right], \tag{3.3}
 \end{aligned}$$

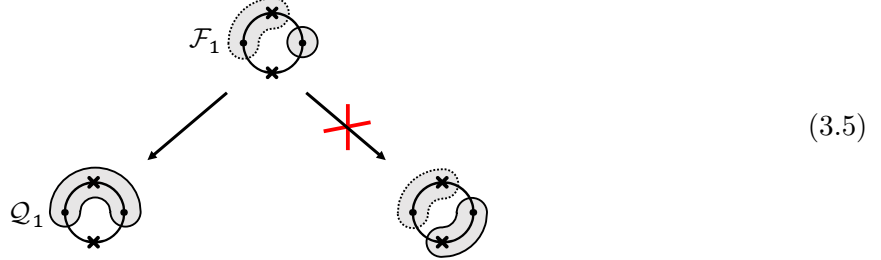
where the letters  $\{l_i\}$  are summarized in table 1.

Then, we move to study the family trees for the source functions  $\mathcal{F}_1$  and  $\tilde{\mathcal{F}}_1$ . For the function  $\mathcal{F}_1$ , the two seeds of  $\mathcal{F}_1$  can be activated independently, forming two different branches:

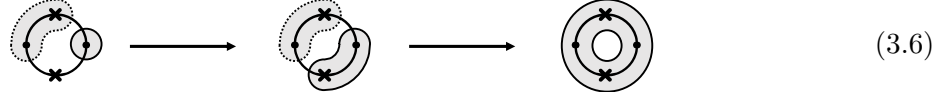


where in the second branch of eq. (3.4), the activated tube can continue to grow and enclose

its adjacent cross signs:

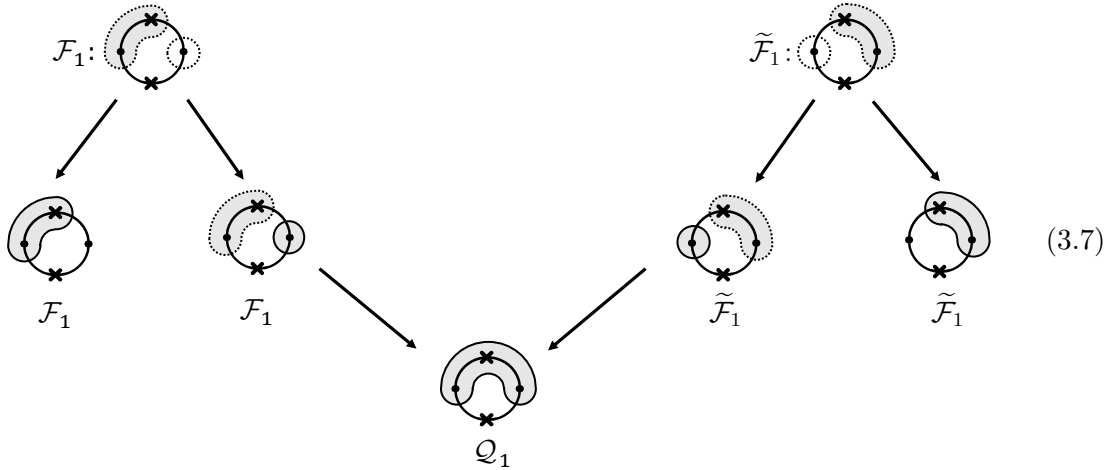


In the second branch of eq. (3.5), the red cross indicates that the activated tube is prevented from eating the adjacent cross sign below it to form this branch. The reason is that if this activated tube were to absorb the cross sign, the newly formed tube would merge with its neighboring tube, yielding to the following family tree

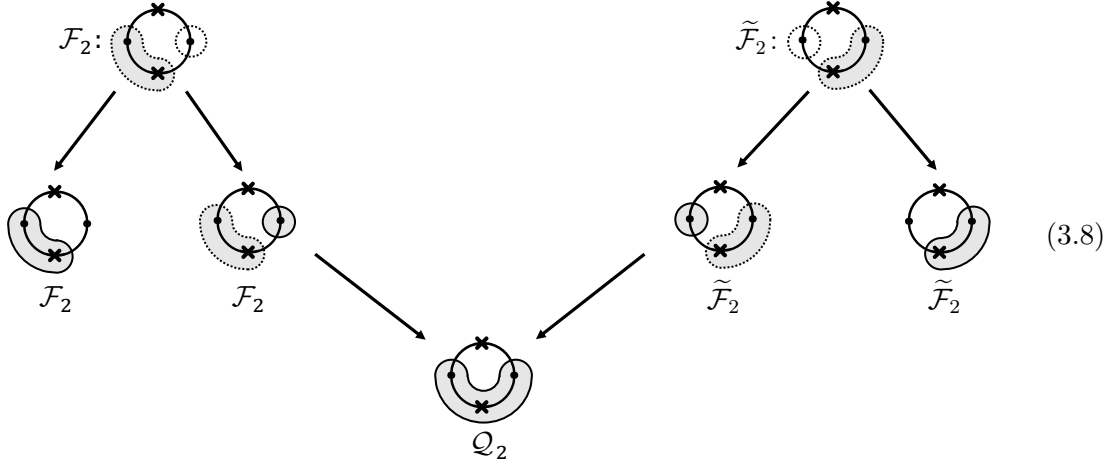


And we can observe that the final descendant tube of (3.6) should correspond to the ultimate tube graph by the family tree of  $\mathcal{F}_3$  and  $\tilde{\mathcal{F}}_3$  in eq. (3.12) (which will be discussed later). Furthermore, the sub-hyperplane arrangement where  $\mathcal{F}_1$  resides is solely related to  $\{T_1, T_2, L_1, L_2, D_1\}$ . However, the final tube graph in eq. (3.6) is related to  $\{T_1, T_2, D_3\}$ , and  $D_3$  clearly should not appear in the sub-hyperplane arrangement system associated with  $\mathcal{F}_1$ . As a result,  $\mathcal{F}_1$  will not evolve along the second branch in eq. (3.6). For the function  $\tilde{\mathcal{F}}_1$ , we can construct its family tree using a method similar to that of  $\mathcal{F}_1$ , so we will ignore the detailed process here.

Therefore, the complete family tree for the functions  $\mathcal{F}_1$  and  $\tilde{\mathcal{F}}_1$  can be constructed as follows:



Similarly, the full family tree for the functions  $\mathcal{F}_2$  and  $\tilde{\mathcal{F}}_2$  is constructed as follows:

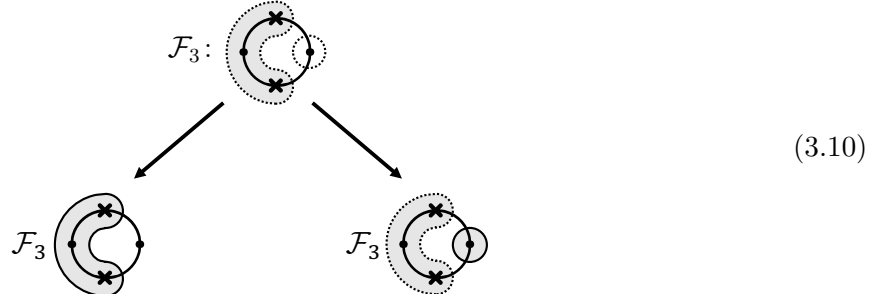


This family trees (3.7)-(3.8) encapsulate the hierarchical relationships between these functions and their derivatives, representing the various levels of their interdependencies. Hence, the differential equations associated with the source functions  $\{\mathcal{F}_1, \tilde{\mathcal{F}}_1, \mathcal{F}_2, \tilde{\mathcal{F}}_2\}$  can be easily read from the family trees (3.7)-(3.8)

$$d\mathcal{F}_1 = \varepsilon [\mathcal{F}_1(l_2 + l_3) + \mathcal{Q}_1(l_9 - l_2)], \quad d\tilde{\mathcal{F}}_1 = \varepsilon [\tilde{\mathcal{F}}_1(l_1 + l_4) + \mathcal{Q}_1(l_9 - l_1)], \quad (3.9a)$$

$$d\mathcal{F}_2 = \varepsilon [\mathcal{F}_2(l_2 + l_5) + \mathcal{Q}_2(l_{10} - l_2)], \quad d\tilde{\mathcal{F}}_2 = \varepsilon [\tilde{\mathcal{F}}_2(l_1 + l_6) + \mathcal{Q}_2(l_{10} - l_1)]. \quad (3.9b)$$

Next, we can concentrate on studying the source functions  $\mathcal{F}_3$  and  $\tilde{\mathcal{F}}_3$ . For  $\mathcal{F}_3$ , there are two seeds in  $\mathcal{F}_3$  and each of them can be activated independently, forming two branches:

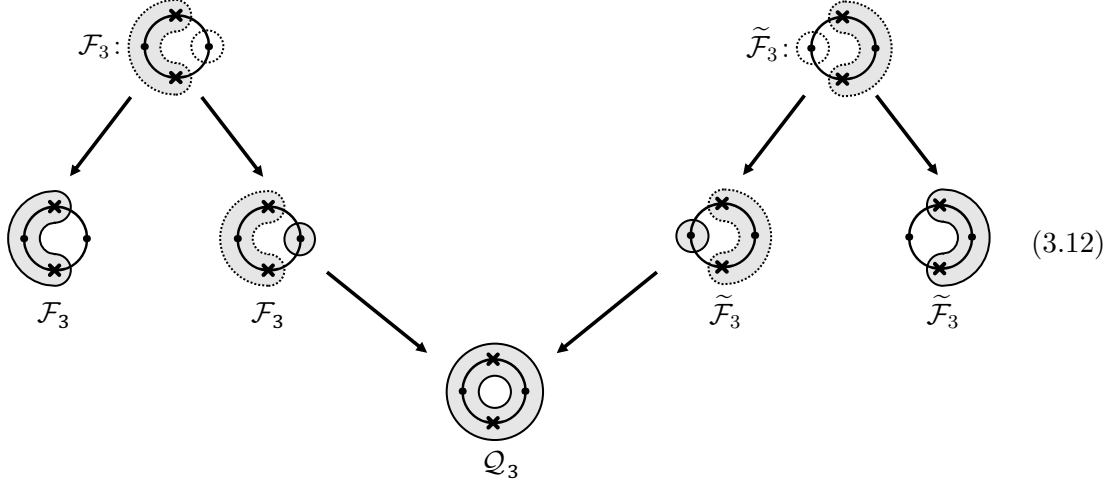


where in the second branch of eq. (3.10), the activated tube can continue to grow and eat all of its adjacent cross signs:



And it is important to note that regardless of whether the tube in the second branch eats the cross above, below, or both, the final result will always be the same tube diagram. A similar approach applies to  $\tilde{\mathcal{F}}_3$ , yielding a comparable diagram. In summary, the full family

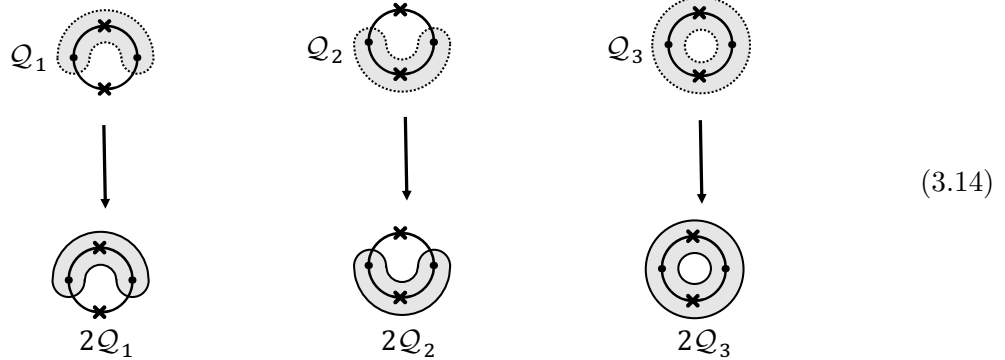
tree associated with  $\mathcal{F}_3$  and  $\tilde{\mathcal{F}}_3$  can be represented as follows:



The differential equations for  $\mathcal{F}_3$  and  $\tilde{\mathcal{F}}_3$  can be obtained from the family tree (3.12) as follows:

$$d\mathcal{F}_3 = \varepsilon [\mathcal{F}_3(l_2 + l_7) + \mathcal{Q}_3(l_{11} - l_2)] , \quad d\tilde{\mathcal{F}}_3 = \varepsilon [\tilde{\mathcal{F}}_3(l_1 + l_8) + \mathcal{Q}_3(l_{11} - l_1)] . \quad (3.13)$$

Finally, we consider the the functions  $\{\mathcal{Q}_i\}$ . In this case, the graphs of  $\mathcal{Q}_i$ 's are enclosed by a single tubing which simply gets activated:



where the factor of two arises from the enclosure of two vertices within the activated tube. Hence, according to the family trees in eq. (3.14), we can obtain the differential equations for  $\mathcal{Q}_1$ ,  $\mathcal{Q}_2$  and  $\mathcal{Q}_3$  as follows:

$$d\mathcal{Q}_1 = 2\varepsilon \mathcal{Q}_1 l_9 , \quad d\mathcal{Q}_2 = 2\varepsilon \mathcal{Q}_2 l_{10} , \quad d\mathcal{Q}_3 = 2\varepsilon \mathcal{Q}_3 l_{11} . \quad (3.15)$$

Collecting all of the differential equations given in eq. (3.3), eq. (3.9) and eq. (3.15), we can verify that the integration family **I**, as constructed, obeys the first-order canonical differential equation presented in eq. (2.10). This indicates that **I** is indeed a canonical basis of master integrals, where each integral exhibits uniform transcendental weight. The

transformation matrix  $\tilde{A}$  is explicitly given by

$$\tilde{A} = \begin{pmatrix} l_1 + l_2 & l_3 - l_1 & l_5 - l_1 & l_7 - l_1 & l_4 - l_2 & l_6 - l_2 & l_8 - l_2 & 0 & 0 & 0 \\ 0 & l_2 + l_3 & 0 & 0 & 0 & 0 & l_9 - l_2 & 0 & 0 & 0 \\ 0 & 0 & l_2 + l_5 & 0 & 0 & 0 & 0 & 0 & l_{10} - l_2 & 0 \\ 0 & 0 & 0 & l_2 + l_7 & 0 & 0 & 0 & 0 & 0 & l_{11} - l_2 \\ 0 & 0 & 0 & 0 & l_1 + l_4 & 0 & 0 & l_9 - l_1 & 0 & 0 \\ 0 & 0 & 0 & 0 & 0 & l_1 + l_6 & 0 & 0 & l_{10} - l_1 & 0 \\ 0 & 0 & 0 & 0 & 0 & 0 & l_1 + l_8 & 0 & 0 & l_{11} - l_1 \\ 0 & 0 & 0 & 0 & 0 & 0 & 0 & 2l_9 & 0 & 0 \\ 0 & 0 & 0 & 0 & 0 & 0 & 0 & 0 & 2l_{10} & 0 \\ 0 & 0 & 0 & 0 & 0 & 0 & 0 & 0 & 0 & 2l_{11} \end{pmatrix}. \quad (3.16)$$

Additionally, it is important to ensure that the system of equations remains consistent. Therefore, we verify that the matrix  $\tilde{A}$  satisfies the integrability conditions (2.11).

Furthermore, we can demonstrate that in the limit  $\varepsilon \rightarrow 0$ , the equations derived in FRW cosmology will reduce to the dS differential equations. By imposing the following rescale in eqs. (3.3), (3.9) and (3.15)

$$\mathcal{F}_i \rightarrow \frac{\mathcal{F}_i^0}{\varepsilon}, \quad \tilde{\mathcal{F}}_i \rightarrow \frac{\tilde{\mathcal{F}}_i^0}{\varepsilon}, \quad \mathcal{Q}_i \rightarrow \frac{\mathcal{Q}_i^0}{\varepsilon^2} \quad (3.17)$$

and taking the limit  $\varepsilon \rightarrow 0$ , we can obtain

$$\begin{aligned} d\mathcal{P}^0 &= \mathcal{F}_1^0(l_3 - l_1) + \tilde{\mathcal{F}}_1^0(l_4 - l_2) + \mathcal{F}_2^0(l_5 - l_1) + \tilde{\mathcal{F}}_2^0(l_6 - l_2) + \mathcal{F}_3^0(l_7 - l_1) + \tilde{\mathcal{F}}_3^0(l_8 - l_2), \\ d\mathcal{F}_1^0 &= \mathcal{Q}_1(l_9 - l_2), \quad d\tilde{\mathcal{F}}_1^0 = \mathcal{Q}_1(l_9 - l_1), \quad d\mathcal{F}_2^0 = \mathcal{Q}_2(l_{10} - l_2), \quad d\tilde{\mathcal{F}}_2^0 = \mathcal{Q}_2(l_{10} - l_1), \\ d\mathcal{F}_3^0 &= \mathcal{Q}_3(l_{11} - l_2), \quad d\tilde{\mathcal{F}}_3^0 = \mathcal{Q}_3(l_{11} - l_1), \quad d\mathcal{Q}_1^0 = d\mathcal{Q}_2^0 = d\mathcal{Q}_3^0 = 0, \end{aligned} \quad (3.18)$$

where they can be uniformly written in the following form:

$$d\mathbf{I}^0 = \varepsilon \tilde{A}^0 \mathbf{I}^0, \quad (3.19)$$

which it is easy to check the transformation matrix in dS space  $\tilde{A}^0$  obeys the integrability conditions (2.11).

Finally, based on the differential equations given in (3.18), we can derive the symbol [15] for two-site one-loop graph in de Sitter spacetime,

$$\begin{aligned} \mathcal{S}_2^{(1)} &= \frac{X_1 + X_2 + 2Y_1}{X_2 + Y_1 + Y_2} \otimes \frac{X_1 + Y_1 - Y_2}{X_1 + Y_1 + Y_2} + \frac{X_1 + X_2 + 2Y_1}{X_1 + Y_1 + Y_2} \otimes \frac{X_2 + Y_1 - Y_2}{X_2 + Y_1 + Y_2} \\ &+ \frac{X_1 + X_2 + 2Y_2}{X_2 + Y_1 + Y_2} \otimes \frac{X_1 - Y_1 + Y_2}{X_1 + Y_1 + Y_2} + \frac{X_1 + X_2 + 2Y_2}{X_1 + Y_1 + Y_2} \otimes \frac{X_2 - Y_1 + Y_2}{X_2 + Y_1 + Y_2} \\ &+ \frac{X_1 + X_2}{X_2 + Y_1 + Y_2} \otimes \frac{X_1 - Y_1 - Y_2}{X_1 + Y_1 + Y_2} + \frac{X_1 + X_2}{X_1 + Y_1 + Y_2} \otimes \frac{X_2 - Y_1 - Y_2}{X_2 + Y_1 + Y_2}, \end{aligned} \quad (3.20)$$

which is analogous to three two-site tree-level chains. Furthermore, our results are consistent with those presented in ref. [4], apart from an overall minus sign that appears in the

third line of eq. (3.20). This difference arises from the conventions used in defining the canonical form. This alignment reinforces the correctness of our method and demonstrates that our approach accurately captures the underlying physical relationships, contributing to a reliable interpretation of the two-site one-loop graph in de Sitter space.

As an additional self-consistency check, we undertake a comparative analysis of the result obtained in (3.16) with it presented in ref. [5]. To facilitate this comparison, we relabel the letters defined in ref. [5] as the letters defined in table 1:

$$\begin{aligned} a_1 &\rightarrow l_{11}, & a_2 &\rightarrow l_9, & a_3 &\rightarrow l_{10}, & a_4 &\rightarrow l_8, & a_5 &\rightarrow l_1, & a_6 &\rightarrow l_2, & a_7 &\rightarrow l_7, \\ a_8 &\rightarrow l_4, & a_9 &\rightarrow l_3, & a_{10} &\rightarrow l_6, & a_{11} &\rightarrow l_5, \end{aligned} \quad (3.21)$$

which allows us to rewrite the matrix obtained by using the dual cohomology method in ref. [5] as:

$$\tilde{A}_{\text{dual}} = \begin{pmatrix} 2l_{11} & 0 & 0 & 0 & 0 & 0 & 0 & 0 & 0 & 0 \\ 0 & 2l_9 & 0 & 0 & 0 & 0 & 0 & 0 & 0 & 0 \\ 0 & 0 & 2l_{10} & 0 & 0 & 0 & 0 & 0 & 0 & 0 \\ l_1 - l_8 & 0 & 0 & l_8 + l_1 & 0 & 0 & 0 & 0 & 0 & 0 \\ l_7 - l_2 & 0 & 0 & 0 & l_2 + l_7 & 0 & 0 & 0 & 0 & 0 \\ 0 & 0 & 0 & 0 & 0 & l_1 + l_2 & 0 & 0 & 0 & 0 \\ 0 & l_4 - l_1 & 0 & 0 & 0 & 0 & l_1 + l_4 & 0 & 0 & 0 \\ 0 & 0 & l_6 - l_1 & 0 & 0 & 0 & 0 & l_1 + l_6 & 0 & 0 \\ 0 & l_2 - l_3 & 0 & 0 & 0 & 0 & 0 & 0 & l_2 + l_3 & 0 \\ 0 & 0 & l_2 - l_5 & 0 & 0 & 0 & 0 & 0 & 0 & l_2 + l_5 \end{pmatrix}. \quad (3.22)$$

By applying a finite series of elementary operations, we find that the expression for  $\tilde{A}$  is equivalent to  $\tilde{A}_{\text{dual}}$ . This agreement provides additional confidence in our methods and highlights the robustness of our findings in relation to established theoretical frameworks.

## 4 Conclusion and Outlook

In this work, we have successfully derived the differential equations for the two-site one-loop graph in the FRW spacetime using relative twisted cohomology and IBP. Our approach, which incorporates kinematic flow and tube graphs, has proven in efficiently obtaining the differential equations. Looking ahead, our future research will focus on extending these methods to higher-loop calculations. Using a similar approach, we provide a brief summary of the differential equations for the sunrise-type two-site two-loop graphs in Appendix B. We hope that this analysis will shed light on the intricate structures underlying these graphs and facilitate further research in the field.

## Acknowledgments

YH is supported in part by the Northwestern University Amplitudes and Insight group, the Department of Physics and Astronomy, and Weinberg College.

## Appendix

### A The Derivation of Two-site One-loop DEs from IBP

#### Differential Forms Bounded by $\{T_1, T_2, L_1, L_2, D_3\} = 0$

Due to its relatively simple structure, we first consider differential forms bounded by  $\{T_1, T_2, L_1, L_2, D_3\} = 0$  and the corresponding functions  $\{\mathcal{P}_3, \mathcal{F}_3, \tilde{\mathcal{F}}_3, \mathcal{Q}_3\}$ . And the total derivative for  $\mathcal{P}_3$  is given by

$$d\mathcal{P}_3 = (\partial_{X_1} \mathcal{P}_3) dX_1 + (\partial_{X_2} \mathcal{P}_3) dX_2 + (\partial_{Y_1} \mathcal{P}_3) dY_1 + (\partial_{Y_2} \mathcal{P}_3) dY_2. \quad (\text{A.1})$$

To obtain the DEs via IBP, we need to trade the derivative of external variables as that of internal variables. For example, the differentiation of external energy  $X_1$  for  $\mathcal{P}_3$  is calculated as

$$\begin{aligned} \partial_{X_1} \mathcal{P}_3 &= \int (x_1 x_2)^\varepsilon \partial_{x_1} \bar{\Omega}_{\mathcal{P}_3} dx_1 \wedge dx_2 \stackrel{\text{IBP}}{=} \varepsilon \int (x_1 x_2)^\varepsilon \left( -\frac{\bar{\Omega}_{\mathcal{P}_3}^2}{T_1} \right) dx_1 \wedge dx_2 \\ &= \varepsilon \int d\mu^\varepsilon \left\{ \left[ \text{Res} \left( -\frac{\bar{\Omega}_{\mathcal{P}_3}^2}{T_1}, D_1=0, D_2=0 \right), \text{Res} \left( -\frac{\bar{\Omega}_{\mathcal{P}_3}^2}{T_1}, T_1=0, D_2=0 \right) \right] \left[ \begin{matrix} \bar{\Omega}_{\mathcal{P}_3}^2 \\ \bar{\Omega}_{\mathcal{F}_3}^2 \end{matrix} \right] \right\} \\ &= \varepsilon \int d\mu^\varepsilon \left[ \frac{\bar{\Omega}_{\mathcal{P}_3}^2}{X_1+Y_1+Y_2} + \frac{2(Y_1+Y_2) \bar{\Omega}_{\mathcal{F}_3}^2}{(X_1-Y_1-Y_2)(X_1+Y_1+Y_2)} \right] \\ &= \varepsilon \left[ \frac{1}{X_1+Y_1+Y_2} \mathcal{P}_3 + \left( \frac{1}{X_1-Y_1-Y_2} - \frac{1}{X_1+Y_1+Y_2} \right) \mathcal{F}_3 \right], \end{aligned} \quad (\text{A.2})$$

where for convenience, we have defined the measure  $d\mu^\varepsilon \equiv (x_1 x_2)^\varepsilon dx_1 \wedge dx_2$ . Similarly, the differentiation with respect to  $X_2$  follows the same steps as for  $X_1$ . And we only need to make the following substitutions:  $X_1 \rightarrow X_2$ ,  $\mathcal{F}_3 \rightarrow \tilde{\mathcal{F}}_3$  in eq. (A.2) to obtain

$$\partial_{X_2} \mathcal{P}_3 = \varepsilon \left[ \frac{1}{X_2+Y_1+Y_2} \mathcal{P}_3 + \left( \frac{1}{X_2-Y_1-Y_2} - \frac{1}{X_2+Y_1+Y_2} \right) \tilde{\mathcal{F}}_3 \right]. \quad (\text{A.3})$$

The differentiation of internal energy  $Y_1$  and  $Y_2$  is somewhat nontrivial. The differentiation of  $Y_1$  for  $\mathcal{P}_3$  can be computed as follows:

$$\begin{aligned} \partial_{Y_1} \mathcal{P}_3 &= \int d\mu^\varepsilon \left[ \partial_{x_1} \left( \frac{-x_1-X_1}{Y_1+Y_2} \bar{\Omega}_{\mathcal{P}_3}^2 \right) + \partial_{x_2} \left( \frac{-x_2-X_2}{Y_1+Y_2} \bar{\Omega}_{\mathcal{P}_3}^2 \right) \right] \\ &= \varepsilon \int d\mu^\varepsilon \left\{ \left[ \text{Res} \left( \frac{(x_1+X_1) \bar{\Omega}_{\mathcal{P}_3}^2}{x_1(Y_1+Y_2)}, D_1=0, D_2=0 \right), \text{Res} \left( \frac{(x_1+X_1) \bar{\Omega}_{\mathcal{P}_3}^2}{x_1(Y_1+Y_2)}, T_1=0, D_2=0 \right) \right] \left[ \begin{matrix} \bar{\Omega}_{\mathcal{P}_3}^2 \\ \bar{\Omega}_{\mathcal{F}_3}^2 \end{matrix} \right] \right. \\ &\quad \left. + \left[ \text{Res} \left( \frac{(x_2+X_2) \bar{\Omega}_{\mathcal{P}_3}^2}{x_2(Y_1+Y_2)}, D_1=0, D_2=0 \right), \text{Res} \left( \frac{(x_2+X_2) \bar{\Omega}_{\mathcal{P}_3}^2}{x_2(Y_1+Y_2)}, T_2=0, D_2=0 \right) \right] \left[ \begin{matrix} \bar{\Omega}_{\mathcal{P}_3}^2 \\ \bar{\Omega}_{\tilde{\mathcal{F}}_3}^2 \end{matrix} \right] \right\} \\ &= \varepsilon \left[ \left( \frac{1}{X_1+Y_1+Y_2} + \frac{1}{X_2+Y_1+Y_2} \right) \mathcal{P}_3 - \left( \frac{1}{X_1+Y_1+Y_2} + \frac{1}{X_1-Y_1-Y_2} \right) \mathcal{F}_3 \right. \\ &\quad \left. - \left( \frac{1}{X_2+Y_1+Y_2} + \frac{1}{X_2-Y_1-Y_2} \right) \tilde{\mathcal{F}}_3 \right]. \end{aligned} \quad (\text{A.4})$$

The calculation for  $Y_2$  is similar to that for  $Y_1$ . By exchanging  $Y_1 \leftrightarrow Y_2$  in eq. (A.4), we can obtain the result for  $Y_2$

$$\begin{aligned}\partial_{Y_2}\mathcal{P}_3 = \partial_{Y_1}\mathcal{P}_3 = \varepsilon \left[ \left( \frac{1}{X_1+Y_1+Y_2} + \frac{1}{X_2+Y_1+Y_2} \right) \mathcal{P}_3 - \left( \frac{1}{X_1+Y_1+Y_2} + \frac{1}{X_1-Y_1-Y_2} \right) \mathcal{F}_3 \right. \\ \left. - \left( \frac{1}{X_2+Y_1+Y_2} + \frac{1}{X_2-Y_1-Y_2} \right) \tilde{\mathcal{F}}_3 \right].\end{aligned}\quad (\text{A.5})$$

In terms of total derivative (A.1) and writing in dlog forms, we can obtain the differential equation for  $\mathcal{P}_3$ :

$$\begin{aligned}d\mathcal{P}_3 = \varepsilon \left[ (\mathcal{P}_3 - \mathcal{F}_3) d\log(X_1 + Y_1 + Y_2) + (\mathcal{P}_3 - \tilde{\mathcal{F}}_3) d\log(X_2 + Y_1 + Y_2) \right. \\ \left. + \mathcal{F}_3 d\log(X_1 - Y_1 - Y_2) + \tilde{\mathcal{F}}_3 d\log(X_2 - Y_1 - Y_2) \right].\end{aligned}\quad (\text{A.6})$$

Next, we examine the differentiation of the source functions  $\mathcal{F}_3$  and  $\tilde{\mathcal{F}}_3$ . For  $\mathcal{F}_3$ , the results with respect to external and internal energy are summarized as follows:

$$\begin{aligned}\partial_{X_1}\mathcal{F}_3 &= \int d\mu^\varepsilon \left[ \partial_{x_1} \left( \frac{-T_1}{X_1 - Y_1 - Y_2} \bar{\Omega}_{\mathcal{F}_3}^2 \right) + \partial_{x_2} \left( \frac{-D_2}{X_1 - Y_1 - Y_2} \bar{\Omega}_{\mathcal{F}_3}^2 \right) \right] \\ &= \varepsilon \int d\mu^\varepsilon \left\{ \left[ \text{Res} \left( \frac{\bar{\Omega}_{\mathcal{F}_3}^2}{X_1 - Y_1 - Y_2}, T_1 = 0, D_2 = 0 \right), \text{Res} \left( \frac{\bar{\Omega}_{\mathcal{F}_3}^2}{X_1 - Y_1 - Y_2}, T_1 = 0, T_2 = 0 \right) \right] \left[ \frac{\bar{\Omega}_{\mathcal{F}_3}^2}{\bar{\Omega}_{\mathcal{Q}_3}^2} \right] \right. \\ &\quad \left. + \left[ \text{Res} \left( \frac{D_2 \bar{\Omega}_{\mathcal{F}_3}^2}{x_2(X_1 - Y_1 - Y_2)}, T_1 = 0, D_2 = 0 \right), \text{Res} \left( \frac{D_2 \bar{\Omega}_{\mathcal{F}_3}^2}{x_2(X_1 - Y_1 - Y_2)}, T_1 = 0, T_2 = 0 \right) \right] \left[ \frac{\bar{\Omega}_{\mathcal{F}_3}^2}{\bar{\Omega}_{\mathcal{Q}_3}^2} \right] \right\} \\ &= \varepsilon \left[ \frac{1}{X_1 - Y_1 - Y_2} \mathcal{F}_3 + \frac{1}{X_1 + X_2} \mathcal{Q}_3 \right],\end{aligned}\quad (\text{A.7a})$$

$$\begin{aligned}\partial_{X_2}\mathcal{F}_3 &= \int d\mu^\varepsilon \partial_{x_2} \bar{\Omega}_{\mathcal{F}_3}^2 \\ &= \varepsilon \left[ \frac{1}{X_2 + Y_1 + Y_2} \mathcal{F}_3 + \left( \frac{1}{X_1 + X_2} - \frac{1}{X_2 + Y_1 + Y_2} \right) \mathcal{Q}_3 \right].\end{aligned}\quad (\text{A.7b})$$

The differentiation with respect to the internal energies is computed as:

$$\begin{aligned}\partial_{Y_1}\mathcal{F}_3 &= \int d\mu^\varepsilon \left[ \partial_{x_1} \left( \frac{x_1}{X_1 - Y_1 - Y_2} \bar{\Omega}_{\mathcal{F}_3}^2 \right) + \partial_{x_2} \left( \frac{x_2 + X_1 + X_2}{X_1 - Y_1 - Y_2} \bar{\Omega}_{\mathcal{F}_3}^2 \right) \right] \\ &= \varepsilon \left[ \left( -\frac{1}{X_1 - Y_1 - Y_2} + \frac{1}{X_2 + Y_1 + Y_2} \right) \mathcal{F}_3 - \frac{1}{X_2 + Y_1 + Y_2} \mathcal{Q}_3 \right],\end{aligned}\quad (\text{A.8a})$$

$$\partial_{Y_2}\mathcal{F}_3 = \partial_{Y_1}\mathcal{F}_3. \quad (\text{A.8b})$$

In terms of total derivative, the differential equations for  $\mathcal{F}_3, \tilde{\mathcal{F}}_3$  are obtained

$$d\mathcal{F}_3 = \varepsilon [\mathcal{F}_3 d\log(X_1 - Y_1 - Y_2) + (\mathcal{F}_3 - \mathcal{Q}_3) d\log(X_2 + Y_1 + Y_2) + \mathcal{Q}_3 d\log(X_1 + X_2)], \quad (\text{A.9})$$

$$d\tilde{\mathcal{F}}_3 = \varepsilon [\tilde{\mathcal{F}}_3 d\log(X_2 - Y_1 - Y_2) + (\tilde{\mathcal{F}}_3 - \mathcal{Q}_3) d\log(X_1 + Y_1 + Y_2) + \mathcal{Q}_3 d\log(X_1 + X_2)]. \quad (\text{A.10})$$

Finally, for the source function  $\mathcal{Q}_3$ , we can derive

$$\begin{aligned}\partial_{X_1}\mathcal{Q}_3 &= \int(x_1x_2)^\varepsilon \left[ \partial_{x_1} \left( \frac{-x_1}{X_1+X_2} \bar{\Omega}_{\mathcal{Q}_3} \right) + \partial_{x_2} \left( \frac{-x_2}{X_1+X_2} \bar{\Omega}_{\mathcal{Q}_3} \right) \right] dx_1 \wedge dx_2 \\ &= 2\varepsilon \left( \frac{1}{X_1+X_2} \right) \mathcal{Q}_3,\end{aligned}\tag{A.11a}$$

$$\partial_{X_2}\mathcal{Q}_3 = 2\varepsilon \left( \frac{1}{X_1+X_2} \right) \mathcal{Q}_3,\tag{A.11b}$$

$$\partial_{Y_1}\mathcal{Q}_3 = \partial_{Y_2}\mathcal{Q}_3 = 0,\tag{A.11c}$$

where the differential equation for  $\mathcal{Q}_3$  is obtained as:

$$d\mathcal{Q}_3 = 2\varepsilon \mathcal{Q}_3 d\log(X_1+X_2).\tag{A.12}$$

### Differential Forms Bounded by $\{T_1, T_2, L_1, L_2, D_1\} = 0$

The differentiation of external energies and internal energies for  $\mathcal{P}_1$  is given by

$$\partial_{X_1}\mathcal{P}_1 = \varepsilon \left[ \frac{1}{X_1+Y_1+Y_2} \mathcal{P}_1 + \left( \frac{1}{X_1+Y_1-Y_2} - \frac{1}{X_1+Y_1+Y_2} \right) \mathcal{F}_1 \right],\tag{A.13a}$$

$$\partial_{X_2}\mathcal{P}_1 = \varepsilon \left[ \frac{1}{X_2+Y_1+Y_2} \mathcal{P}_1 + \left( \frac{1}{X_2+Y_1-Y_2} - \frac{1}{X_2+Y_1+Y_2} \right) \tilde{\mathcal{F}}_1 \right],\tag{A.13b}$$

$$\begin{aligned}\partial_{Y_1}\mathcal{P}_1 &= \int d\mu^\varepsilon \left( \partial_{x_1} \bar{\Omega}_{\mathcal{P}_1}^2 + \partial_{x_2} \bar{\Omega}_{\mathcal{P}_1}^2 \right) \\ &= \varepsilon \left[ \left( \frac{1}{X_1+Y_1+Y_2} + \frac{1}{X_2+Y_1+Y_2} \right) \mathcal{P}_1 + \left( \frac{1}{X_1+Y_1-Y_2} - \frac{1}{X_1+Y_1+Y_2} \right) \mathcal{F}_1 \right. \\ &\quad \left. + \left( \frac{1}{X_2+Y_1-Y_2} - \frac{1}{X_2+Y_1+Y_2} \right) \tilde{\mathcal{F}}_1 \right],\end{aligned}\tag{A.13c}$$

$$\begin{aligned}\partial_{Y_2}\mathcal{P}_1 &= \int d\mu^\varepsilon \left[ \partial_{x_1} \left( \frac{-x_1-X_1-Y_1}{Y_2} \bar{\Omega}_{\mathcal{P}_1}^2 \right) + \partial_{x_2} \left( \frac{-x_2-X_2-Y_2}{Y_2} \bar{\Omega}_{\mathcal{P}_1}^2 \right) \right] \\ &= \varepsilon \left[ \left( \frac{1}{X_1+Y_1+Y_2} + \frac{1}{X_2+Y_1+Y_2} \right) \mathcal{P}_1 + \left( -\frac{1}{X_1+Y_1-Y_2} - \frac{1}{X_1+Y_1+Y_2} \right) \mathcal{F}_1 \right. \\ &\quad \left. + \left( -\frac{1}{X_2+Y_1-Y_2} - \frac{1}{X_2+Y_1+Y_2} \right) \tilde{\mathcal{F}}_1 \right],\end{aligned}\tag{A.13d}$$

where in terms of total derivative, we have

$$\begin{aligned}d\mathcal{P}_1 &= \varepsilon [(\mathcal{P}_1 - \mathcal{F}_1) d\log(X_1+Y_1+Y_2) + (\mathcal{P}_1 - \tilde{\mathcal{F}}_1) d\log(X_2+Y_1+Y_2) \\ &\quad + \mathcal{F}_1 d\log(X_1+Y_1-Y_2) + \tilde{\mathcal{F}}_1 d\log(X_2+Y_1-Y_2)].\end{aligned}\tag{A.14}$$

For the source functions  $\mathcal{F}_1$  and  $\tilde{\mathcal{F}}_1$ , we can calculate

$$\begin{aligned}\partial_{X_1}\mathcal{F}_1 &= \int d\mu^\varepsilon \left[ \partial_{x_1} \left( \frac{-x_1}{X_1+Y_1-Y_2} \bar{\Omega}_{\mathcal{F}_1}^2 \right) + \partial_{x_2} \left( \frac{-D_2}{X_1+Y_1-Y_2} \bar{\Omega}_{\mathcal{F}_1}^2 \right) \right] \\ &= \varepsilon \left[ \frac{1}{X_1+Y_1-Y_2} \mathcal{F}_1 + \frac{1}{X_1+X_2+2Y_1} \mathcal{Q}_1 \right],\end{aligned}\tag{A.15a}$$

$$\partial_{X_2}\mathcal{F}_1 = \varepsilon \left[ \frac{1}{X_2+Y_1+Y_2} \mathcal{F}_1 + \left( \frac{1}{X_1+X_2+2Y_1} - \frac{1}{X_2+Y_1+Y_2} \right) \mathcal{Q}_1 \right],\tag{A.15b}$$

$$\begin{aligned}\partial_{Y_1}\mathcal{F}_1 &= \int d\mu^\varepsilon \left[ \partial_{x_1} \left( \frac{-x_1}{X_1+Y_1-Y_2} \bar{\Omega}_{\mathcal{F}_1}^2 \right) + \partial_{x_2} \left( \frac{-x_2+X_1-X_2-2Y_2}{X_1+Y_1-Y_2} \bar{\Omega}_{\mathcal{F}_1}^2 \right) \right] \\ &= \varepsilon \left[ \left( \frac{1}{X_1+Y_1-Y_2} + \frac{1}{X_2+Y_1+Y_2} \right) \mathcal{F}_1 + \left( \frac{2}{X_1+X_2+2Y_1} - \frac{1}{X_2+Y_1+Y_2} \right) \mathcal{Q}_1 \right],\end{aligned}\quad (\text{A.15c})$$

$$\begin{aligned}\partial_{Y_2}\mathcal{F}_1 &= \int d\mu^\varepsilon \left[ \partial_{x_1} \left( \frac{-x_1}{X_1+Y_1-Y_2} \bar{\Omega}_{\mathcal{F}_1}^2 \right) + \partial_{x_2} \left( \frac{x_2+X_1+X_2+2Y_2}{X_1+Y_1-Y_2} \bar{\Omega}_{\mathcal{F}_1}^2 \right) \right] \\ &= \varepsilon \left[ \left( -\frac{1}{X_1+Y_1-Y_2} + \frac{1}{X_2+Y_1+Y_2} \right) \mathcal{F}_1 - \frac{1}{X_2+Y_1+Y_2} \mathcal{Q}_1 \right],\end{aligned}\quad (\text{A.15d})$$

where in terms of total derivative, we can obtain the following differential equations

$$\begin{aligned}d\mathcal{F}_1 &= \varepsilon [\mathcal{F}_1 d\log(X_1+Y_1-Y_2) + (\mathcal{F}_1 - \mathcal{Q}_1) d\log(X_2+Y_1+Y_2) \\ &\quad + \mathcal{Q}_1 d\log(X_1+X_2+2Y_1)],\end{aligned}\quad (\text{A.16a})$$

$$\begin{aligned}d\tilde{\mathcal{F}}_1 &= \varepsilon [\tilde{\mathcal{F}}_1 d\log(X_2+Y_1-Y_2) + (\tilde{\mathcal{F}}_1 - \mathcal{Q}_1) d\log(X_1+Y_1+Y_2) \\ &\quad + \mathcal{Q}_1 d\log(X_1+X_2+2Y_1)].\end{aligned}\quad (\text{A.16b})$$

And for  $\mathcal{Q}_1$ , we compute

$$\begin{aligned}\partial_{X_1}\mathcal{Q}_1 &= \int d\mu^\varepsilon \left[ \partial_{x_1} \left( \frac{-x_1}{X_1+X_2+2Y_1} \bar{\Omega}_{\mathcal{Q}_1}^2 \right) + \partial_{x_2} \left( \frac{-x_2}{X_1+X_2+2Y_1} \bar{\Omega}_{\mathcal{Q}_1}^2 \right) \right], \\ &= 2\varepsilon \left( \frac{1}{X_1+X_2+2Y_1} \right) \mathcal{Q}_1,\end{aligned}\quad (\text{A.17a})$$

$$\partial_{X_2}\mathcal{Q}_1 = 2\varepsilon \left( \frac{1}{X_1+X_2+2Y_1} \right) \mathcal{Q}_1,\quad (\text{A.17b})$$

$$\begin{aligned}\partial_{Y_1}\mathcal{Q}_1 &= \int d\mu^\varepsilon \left[ \partial_{x_1} \left( \frac{-2x_1}{X_1+X_2+2Y_1} \bar{\Omega}_{\mathcal{Q}_1}^2 \right) + \partial_{x_2} \left( \frac{-2x_2}{X_1+X_2+2Y_1} \bar{\Omega}_{\mathcal{Q}_1}^2 \right) \right] \\ &= \frac{4\varepsilon}{X_1+X_2+2Y_1} \mathcal{Q}_1,\end{aligned}\quad (\text{A.17c})$$

$$\partial_{Y_2}\mathcal{Q}_1 = 0.\quad (\text{A.17d})$$

where the differential equation for  $\mathcal{Q}_1$  is obtained as:

$$d\mathcal{Q}_1 = 2\varepsilon \mathcal{Q}_1 d\log(X_1+X_2+2Y_1).\quad (\text{A.18})$$

**Differential Forms Bounded by  $\{T_1, T_2, L_1, L_2, D_2\} = 0$**

The differential equations for  $\{\mathcal{P}_2, \mathcal{F}_2, \tilde{\mathcal{F}}_2, \mathcal{Q}_2\}$  are obtained by exchanging  $Y_1 \leftrightarrow Y_2$  in the differential equations for  $\{\mathcal{P}_1, \mathcal{F}_1, \tilde{\mathcal{F}}_1, \mathcal{Q}_1\}$ , which are summarized as follows:

$$\begin{aligned}d\mathcal{P}_2 &= \varepsilon [(\mathcal{P}_2 - \mathcal{F}_2) d\log(X_1+Y_1+Y_2) + (\mathcal{P}_2 - \tilde{\mathcal{F}}_2) d\log(X_2+Y_1+Y_2) \\ &\quad + \mathcal{F}_2 d\log(X_1-Y_1+Y_2) + \tilde{\mathcal{F}}_2 d\log(X_2-Y_1+Y_2)],\end{aligned}\quad (\text{A.19a})$$

$$\begin{aligned}d\mathcal{F}_2 &= \varepsilon [\mathcal{F}_2 d\log(X_1-Y_1+Y_2) + (\mathcal{F}_2 - \mathcal{Q}_2) d\log(X_2+Y_1+Y_2) \\ &\quad + \mathcal{Q}_2 d\log(X_1+X_2+2Y_2)],\end{aligned}\quad (\text{A.19b})$$

$$d\tilde{\mathcal{F}}_2 = \varepsilon [\tilde{\mathcal{F}}_2 d\log(X_2-Y_1+Y_2) + (\tilde{\mathcal{F}}_2 - \mathcal{Q}_2) d\log(X_1+Y_1+Y_2)]$$

$$+ \mathcal{Q}_2 \text{dlog}(X_2 + X_2 + 2Y_2) \big] , \quad (\text{A.19c})$$

$$\text{d}\mathcal{Q}_2 = 2\varepsilon \mathcal{Q}_2 \text{dlog}(X_1 + X_2 + 2Y_2) . \quad (\text{A.19d})$$

Finally, we group  $\mathcal{P}_1$ ,  $\mathcal{P}_2$ , and  $\mathcal{P}_3$  together as  $\mathcal{P} = \sum_{i=1}^3 \mathcal{P}_i$ , yielding to the total derivative:

$$\begin{aligned} \text{d}\mathcal{P} = \varepsilon & \left[ \left( \mathcal{P} - \sum_{i=1}^3 \mathcal{F}_i \right) \text{dlog}(X_1 + Y_1 + Y_2) + \left( \mathcal{P} - \sum_{i=1}^3 \tilde{\mathcal{F}}_i \right) \text{dlog}(X_2 + Y_1 + Y_2) \right. \\ & + \mathcal{F}_1 \text{dlog}(X_1 + Y_1 - Y_2) + \tilde{\mathcal{F}}_1 \text{dlog}(X_2 + Y_1 - Y_2) \\ & + \mathcal{F}_2 \text{dlog}(X_1 - Y_1 + Y_2) + \tilde{\mathcal{F}}_2 \text{dlog}(X_2 - Y_1 + Y_2) \\ & \left. + \mathcal{F}_3 \text{dlog}(X_1 - Y_1 - Y_2) + \tilde{\mathcal{F}}_3 \text{dlog}(X_2 - Y_1 - Y_2) \right] . \end{aligned} \quad (\text{A.20})$$

## B Differential Equations for Two-site Two-loop Graph

In  $\phi^4$  theory, the Feynman diagram for two-site two-loop (sunrise) wavefunction coefficient is given in fig. 3. The wavefunction coefficient in the FRW spacetime is

$$\psi_2^{(2)} = \int dx_1 \wedge dx_2 \frac{(T_1 T_2)^\varepsilon}{L_1 L_2 D_7} \left[ \frac{1}{D_1} \left( \frac{1}{D_4} + \frac{1}{D_5} \right) + \frac{1}{D_2} \left( \frac{1}{D_4} + \frac{1}{D_6} \right) + \frac{1}{D_3} \left( \frac{1}{D_5} + \frac{1}{D_6} \right) \right] , \quad (\text{B.1})$$

where we have defined the divisors as follows:

$$\begin{aligned} T_1 &= x_1 , \quad T_2 = x_2 , \\ L_1 &= X_1 + x_1 + \sum_{i=1}^3 Y_i , \quad L_2 = X_2 + x_2 + \sum_{i=1}^3 Y_i , \\ D_1 &= X_1 + X_2 + x_1 + x_2 + 2Y_1 , \quad D_2 = X_1 + X_2 + x_1 + x_2 + 2Y_2 , \\ D_3 &= X_1 + X_2 + x_1 + x_2 + 2Y_3 , \quad D_4 = X_1 + X_2 + x_1 + x_2 + 2(Y_1 + Y_2) , \\ D_5 &= X_1 + X_2 + x_1 + x_2 + 2(Y_1 + Y_3) , \quad D_6 = X_1 + X_2 + x_1 + x_2 + 2(Y_2 + Y_3) , \\ D_7 &= X_1 + X_2 + x_1 + x_2 . \end{aligned} \quad (\text{B.2})$$

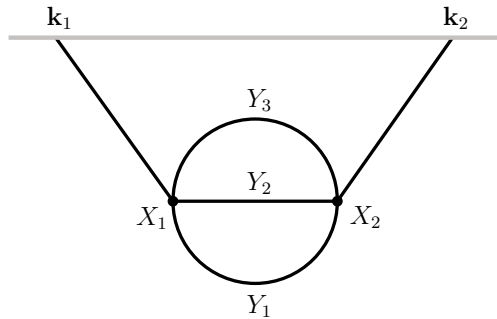


**Figure 3.** The Feynman diagram for the two-site two-loop wavefunction coefficient.

There are 22 members in the integration family **I** and the differential equations for **I** are given by

$$\begin{aligned}
d\mathcal{P} &= \varepsilon[\mathcal{P}(l_1 + l_2) + \sum_{a=1}^7 \mathcal{F}_a(l_{2a+1} - l_1) + \sum_{a=1}^7 \tilde{\mathcal{F}}_a(l_{2a+2} - l_2)], \\
d\mathcal{F}_i &= \varepsilon[\mathcal{F}_i(l_{2i+1} + l_2) + \mathcal{Q}_i(l_{i+16} - l_2)], \\
d\tilde{\mathcal{F}}_i &= \varepsilon[\tilde{\mathcal{F}}_i(l_{2i+2} + l_1) + \mathcal{Q}_i(l_{i+16} - l_1)], \\
d\mathcal{Q}_i &= 2\varepsilon\mathcal{Q}_i l_{i+16},
\end{aligned} \tag{B.3}$$

where  $i = 1, \dots, 7$  and the letters are summarized in table 2.

$l_1$		$d\log(X_1 + Y_1 + Y_2 + Y_3)$	$l_2$		$d\log(X_2 + Y_1 + Y_2 + Y_3)$
$l_3$		$d\log(X_1 + Y_1 + Y_2 - Y_3)$	$l_4$		$d\log(X_2 + Y_1 + Y_2 - Y_3)$
$l_5$		$d\log(X_1 + Y_1 - Y_2 + Y_3)$	$l_6$		$d\log(X_2 + Y_1 - Y_2 + Y_3)$
$l_7$		$d\log(X_1 - Y_1 + Y_2 + Y_3)$	$l_8$		$d\log(X_2 - Y_1 + Y_2 + Y_3)$
$l_9$		$d\log(X_1 + Y_1 - Y_2 - Y_3)$	$l_{10}$		$d\log(X_2 + Y_1 - Y_2 - Y_3)$
$l_{11}$		$d\log(X_1 - Y_1 + Y_2 - Y_3)$	$l_{12}$		$d\log(X_2 - Y_1 + Y_2 - Y_3)$
$l_{13}$		$d\log(X_1 - Y_1 - Y_2 + Y_3)$	$l_{14}$		$d\log(X_2 - Y_1 - Y_2 + Y_3)$
$l_{15}$		$d\log(X_1 - Y_1 - Y_2 - Y_3)$	$l_{16}$		$d\log(X_2 - Y_1 - Y_2 - Y_3)$
$l_{17}$		$d\log(X_1 + X_2 + 2Y_1 + 2Y_2)$	$l_{18}$		$d\log(X_1 + X_2 + 2Y_1 + 2Y_3)$
$l_{19}$		$d\log(X_1 + X_2 + 2Y_2 + 2Y_3)$	$l_{20}$		$d\log(X_1 + X_2 + 2Y_1)$
$l_{21}$		$d\log(X_1 + X_2 + 2Y_2)$	$l_{22}$		$d\log(X_1 + X_2 + 2Y_3)$
$l_{23}$		$d\log(X_1 + X_2)$			

**Table 2.** The alphabet of two-site one-loop wavefunction coefficient where  $l_i \equiv d\log \ell_i$ .

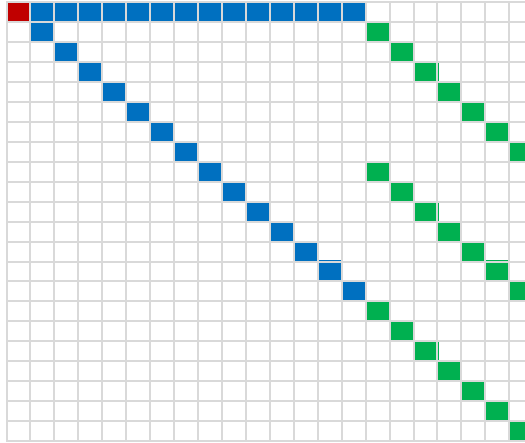


**Figure 4.** Transformation matrix for two-site two-loop diagram.

Further, the differential equations (B.3) are uniformly expressed in the following form:

$$d\mathbf{I} = \varepsilon \tilde{A} \mathbf{I}, \quad \mathbf{I} = (\mathcal{P}, \mathcal{F}_1, \dots, \mathcal{F}_7, \tilde{\mathcal{F}}_1, \dots, \tilde{\mathcal{F}}_7, \mathcal{Q}_1, \dots, \mathcal{Q}_7)^T, \quad (\text{B.4})$$

where the matrix  $\tilde{A}$ , illustrated in fig. 4, can be verified to obey the conditions (2.11).

## References

- [1] N. Arkani-Hamed, P. Benincasa, and A. Postnikov, “Cosmological Polytopes and the Wavefunction of the Universe,” [arXiv:1709.02813 \[hep-th\]](https://arxiv.org/abs/1709.02813).
- [2] N. Arkani-Hamed and P. Benincasa, “On the Emergence of Lorentz Invariance and Unitarity from the Scattering Facet of Cosmological Polytopes,” [arXiv:1811.01125 \[hep-th\]](https://arxiv.org/abs/1811.01125).
- [3] P. Benincasa, “From the flat-space S-matrix to the Wavefunction of the Universe,” [arXiv:1811.02515 \[hep-th\]](https://arxiv.org/abs/1811.02515).
- [4] A. Hillman, “Symbol Recursion for the dS Wave Function,” [arXiv:1912.09450 \[hep-th\]](https://arxiv.org/abs/1912.09450).
- [5] S. De and A. Pokraka, “Cosmology meets cohomology,” *JHEP* **03** (2024) 156, [arXiv:2308.03753 \[hep-th\]](https://arxiv.org/abs/2308.03753).
- [6] N. Arkani-Hamed, D. Baumann, A. Hillman, A. Joyce, H. Lee, and G. L. Pimentel, “Kinematic Flow and the Emergence of Time,” [arXiv:2312.05300 \[hep-th\]](https://arxiv.org/abs/2312.05300).
- [7] N. Arkani-Hamed, D. Baumann, A. Hillman, A. Joyce, H. Lee, and G. L. Pimentel, “Differential Equations for Cosmological Correlators,” [arXiv:2312.05303 \[hep-th\]](https://arxiv.org/abs/2312.05303).
- [8] K. Aomoto and M. Kita, *Theory of Hypergeometric Functions*. Springer Monographs in Mathematics. Springer, 2011.
- [9] M. Yoshida, *Hypergeometric Functions, My Love: Modular Interpretations of Configuration Spaces*. Aspects of Mathematics. Vieweg+Teubner Verlag, 2013. <https://books.google.com/books?id=hYQECAAAQBAJ>.
- [10] K. Aomoto, “On vanishing of cohomology attached to certain many valued meromorphic functions,” *Journal of the Mathematical Society of Japan* **27** no. 2, (1975) 248–255.

- [11] P. Mastrolia and S. Mizera, “Feynman Integrals and Intersection Theory,” *JHEP* **02** (2019) 139, [arXiv:1810.03818 \[hep-th\]](https://arxiv.org/abs/1810.03818).
- [12] N. Arkani-Hamed, Y. Bai, and T. Lam, “Positive Geometries and Canonical Forms,” *JHEP* **11** (2017) 039, [arXiv:1703.04541 \[hep-th\]](https://arxiv.org/abs/1703.04541).
- [13] H. Frellesvig, F. Gasparotto, S. Laporta, M. K. Mandal, P. Mastrolia, L. Mattiazzi, and S. Mizera, “Decomposition of Feynman Integrals on the Maximal Cut by Intersection Numbers,” *JHEP* **05** (2019) 153, [arXiv:1901.11510 \[hep-ph\]](https://arxiv.org/abs/1901.11510).
- [14] J. M. Henn, “Multiloop integrals in dimensional regularization made simple,” *Phys. Rev. Lett.* **110** (2013) 251601, [arXiv:1304.1806 \[hep-th\]](https://arxiv.org/abs/1304.1806).
- [15] A. B. Goncharov, M. Spradlin, C. Vergu, and A. Volovich, “Classical Polylogarithms for Amplitudes and Wilson Loops,” *Phys. Rev. Lett.* **105** (2010) 151605, [arXiv:1006.5703 \[hep-th\]](https://arxiv.org/abs/1006.5703).